Equilibrium speciation dynamics in a model adaptive radiation of island lizards

Daniel L. Rabosky[a,b,1] and Richard E. Glor[c]

[a]Department of Ecology and Evolutionary Biology and Laboratory of Ornithology, Cornell University, Ithaca, NY 14853; [b]Department of Integrative Biology and Museum of Vertebrate Zoology, University of California, Berkeley, CA 94720; and [c]Department of Biology, University of Rochester, Rochester, NY 14620

Edited* by David B. Wake, University of California, Berkeley, CA, and approved November 5, 2010 (received for review May 30, 2010)

The relative importance of equilibrium and nonequilibrium processes in shaping patterns of species richness is one of the most fundamental questions in biodiversity studies. If equilibrium processes predominate, then ecological interactions presumably limit species diversity, potentially through diversity dependence of immigration, speciation, and extinction rates. Alternatively, species richness may be limited by the rate at which diversity arises or by the amount of time available for diversification. These latter explanations constitute nonequilibrium processes and can apply only to biotas that are unsaturated or far from diversity equilibria. Recent studies have challenged whether equilibrium models apply to biotas assembled through in situ speciation, as this process may be too slow to achieve steady-state diversities. Here we demonstrate that speciation rates in replicate Caribbean lizard radiations have undergone parallel declines to equilibrium conditions on three of four major islands. Our results suggest that feedback between total island diversity and per-capita speciation rates scales inversely with island area, with proportionately greater declines occurring on smaller islands. These results are consistent with strong ecological controls on species richness and suggest that the iconic adaptive radiation of Caribbean anoles may have reached an endpoint.

island biogeography | macroevolution | species-area relationship | ecological limits | phylogeny

Under MacArthur and Wilson's equilibrium model of island biogeography (1), a positive relationship between an island's area and its species diversity arises from a dynamic balance between the rate at which new species colonize an area and the rate at which species are lost due to extinction. For a given degree of isolation, larger islands should contain more species than smaller islands because they have lower rates of extinction and, potentially, increased rates of colonization. Although this model is clearly a simplification of processes influencing species richness (2, 3), it has nonetheless retained considerable explanatory power (2, 4, 5).

A number of recent analyses, however, suggest that nonequilibrium dynamics might prevail when speciation, as opposed to immigration, is the principal contributor to species richness (6, 7). In some systems, speciation rates may be too low relative to the age of a given island or geographic region to achieve equilibrium species numbers (6–8). In other cases, extinction pulses might occur with sufficient frequency that diversity never reaches equilibrium (9). Because speciation dominates the assembly of biotas on large islands and continents, understanding many patterns of species richness potentially requires a nonequilibrium, evolutionary theory of diversity. Such a nonequilibrium model of diversity would entail primary control of species richness by variation in net diversification rates, clade age, or time within regions (10–14).

Alternatively, species richness might be governed by a logistic growth process (15, 16), such that speciation and extinction rates reach a balance only when some island- or region-specific carrying capacity has been achieved. These models have been widely used in paleobiological studies to explain diversity dynamics at the largest temporal and spatial scales (17, 18), and some recent studies on dated phylogenetic trees support speciation rate decline over time during evolutionary radiations, perhaps due to saturation of ecological niches with increasing species richness (19, 20). However, the evidence for equilibrium dynamics from more restricted phylogenetic and spatial scales is generally mixed, particularly for islands (7, 21–23).

The species diversity of reptiles and amphibians observed across the West Indian archipelago has been used to support both equilibrium, immigration-based and nonequilibrium, speciation-based explanations for the species–area relationship (1, 7, 24). Here, we test whether equilibrium or nonequilibrium macroevolutionary models best characterize patterns of diversification in the archipelago's most diverse lizard genus (*Anolis*). We focus on anole radiations that have occurred on the four large islands of the Greater Antilles (Cuba, Hispaniola, Jamaica, and Puerto Rico), which resulted primarily from in situ speciation (7). Previous analyses suggested that speciation rates in Caribbean anoles reflect far-from-equilibrium dynamics, with relatively constant but island-specific diversification rates through time (7, 25). These results suggest that, at least for anoles, species richness within islands is limited by the rate at which diversity arises (e.g., the difference between the speciation rate, λ, and the extinction rate, μ) and not by ecological limits on diversification or island-specific carrying capacities (14). However, the nonequilibrium model has never been tested using methods that explicitly allow for temporal variation in rates of species diversification through time. If net diversification rates ($\lambda - \mu$) in *Anolis* follow the equilibrium model, we predict that (*i*) island-specific declines in diversification should occur on each of the four major islands of the Greater Antilles and (*ii*) rates should decline more quickly to an equilibrium on smaller islands, consistent with the hypothesis that small islands have lower carrying capacities than large islands.

Results

We used the state-dependent speciation-extinction (SSE) framework that has previously been used to study the relationship between character states and diversification rates (26–28), extended to include dynamic processes of character change, speciation, and extinction. The binary-state (BiSSE) model (27) describes the probability that a lineage in state k at some point in time will evolve into a clade identical to the observed clade, given a particular set of speciation (λ_0, λ_1), extinction (μ_0, μ_1), and character transition (q_{01}, q_{10}) parameters. By assuming that lineage dispersal between islands can be modeled as a transition between character states on a phylogenetic tree, we can use a generalization of this model to study the dynamics of diversification in Caribbean anoles. Let $D_i(t)$ be the probability that

Author contributions: D.L.R. and R.E.G. designed research, performed research, contributed new reagents/analytic tools, analyzed data, and wrote the paper.

The authors declare no conflict of interest.

*This Direct Submission article had a prearranged editor.

[1]To whom correspondence should be addressed. E-mail: drabosky@berkeley.edu.

This article contains supporting information online at www.pnas.org/lookup/suppl/doi:10.1073/pnas.1007606107/-/DCSupplemental.

a lineage in state i at time t evolves into a clade identical to the observed clade, and let $E_i(t)$ be the corresponding probability of clade extinction before the present. For each character state, we obtain a pair of differential equations that describe changes in $D_i(t)$ and $E_i(t)$ through time,

$$\frac{dD_i}{dt} = -\left(\mu_{i,t} + \lambda_{i,t} + \sum_{j=1}^{j\neq i} q_{ij,t}\right)D_i(t) + \sum_{j=1}^{j\neq i} q_{ij,t}D_j(t) + 2\lambda_{i,t}E_i(t)D_i(t)$$

and

$$\frac{dE_i}{dt} = \mu_{i,t} - \left(\mu_{i,t} + \lambda_{i,t} + \sum_{j=1}^{j\neq i} q_{ij,t}\right)E_i(t) + \sum_{j=1}^{j\neq i} q_{ij,t}E_j(t) + \lambda_{i,t}E_i(t)^2,$$

where $\lambda_{i,t}$ and $\mu_{i,t}$ are the rates of speciation and extinction for the ith character state at time t, and where $q_{ij,t}$ is the rate of character change from state i to state j at time t. For n character states, computing the probability of the observed data given the model and parameters requires that we solve $2n$ ordinary differential equations that jointly describe the dynamics of speciation, extinction, and state change along each branch of a phylogenetic tree (*SI Materials and Methods*). We assume that rates of speciation, extinction, and dispersal change linearly through time, such that

$$r(\tau) = \max\left\{0,\ r_0\left(1 - \frac{\tau}{K}\right)\right\},$$

where r_0 is the initial rate at the root node of the complete tree ($\lambda_{i,0}$, $\mu_{i,0}$, or $q_{ij,0}$), τ is time measured from the root node, and K controls the rate of change in speciation, extinction, or dispersal through time.

We applied this framework to a phylogenetic tree for Greater Antillean *Anolis* (29) that was 88% complete at the species level (Figs. S1 and S2) and modified initial values for D_i and E_i to account for incomplete taxon sampling. Implementation of the model requires an appropriate rate matrix describing possible dispersals between islands (e.g., $q_{ij,t} = q$ for a one-rate, time-constant symmetric model). We used maximum likelihood to evaluate 12 alternative time-constant or time-varying dispersal models (*Materials and Methods*, *SI Materials and Methods*, Table S1, and Fig. S3). Models with temporal declines in the rate of dispersal between islands fit the data much better than those with time-invariant dispersal (ΔAIC = 19.2 in favor of models with temporal variation in q; Table S1). This result may also be consistent with the possibility that between-island speciation events reflect early vicariance of Antillean proto-islands, rather than among-island dispersal (30).

We then incorporated this "background" biogeographic model into a series of diversification models that allowed speciation and extinction dynamics to vary among islands. Our candidate set of models included a model with a common time-invariant speciation rate (λ) across all islands (model 1: GlobalConstant), a model with island-specific but time-invariant λ (model 2: IslandConstant), a model with "global" changes in diversification rate (model 3: GlobalVariable), and two models with island-specific linear change in λ through time (model 4: IslandVariable; and model 5: IslandVariableFull). The IslandVariableFull model has separate λ_0 and K parameters for each island, whereas IslandVariable is a reduced model with a common starting rate λ_0 at the root node of the tree. For each model of speciation described above, we considered variants with and without extinction (*Materials and Methods*).

The GlobalVariable model describes a scenario where speciation rates across the entire Greater Antillean radiation have changed with a common underlying dynamic that is independent of the island to which each lineage belongs. Including these models enables us to distinguish island-specific dynamics from well-known biases that can lead phylogenetic studies to infer spurious declines in speciation rates through time (19, 31, 32). If apparent rapid speciation at the base of a phylogeny is an artifact of tree construction, sampling biases, and inadequate models of molecular evolution, we should observe superior fit of the GlobalVariable model. This model would also be expected to fit the data well if diversification rates have changed during the course of the anole radiation in response to a common climatic driver.

Our results strongly reject the hypothesis that island-specific but time-invariant diversification underlies patterns of anole species richness in the Greater Antilles (Table 1). The conditional probability of the two constant rate models (*Materials and Methods*) is very low ($P < 0.0001$). Rather, our results support the hypothesis that speciation rates have declined independently on each island (Fig. 1), against a background of low extinction (Table 1). The best-fit model specified independent linear declines in the rate of speciation on each island (IslandVariable; conditional probability = 0.811), and the second-best model was the IslandVariableFull model ($P = 0.184$). Together, these island-specific decline models account for 0.995 of the total probability of the data explained by the candidate set of models and do not support the hypothesis that lineage accumulation patterns in *Anolis* reflect global drivers of diversification or artifacts of tree construction. If the IslandVariableFull model is excluded, the conditional probability of the IslandVariable model is very high ($P = 0.994$). These results are robust to phylogenetic uncertainty (Fig. S4); virtually identical results are obtained under alternative biogeographic models, including a simple model with symmetric time-invariant dispersal rates between islands (Table S2). Models without extinction consistently fit the data better than the corresponding models with extinction (Table 1).

We estimated occupancy probabilities and lineage accumulation curves for each island under the best-fit diversification model (Fig. 2); these curves suggest relatively rapid accumulation of lineages on Hispaniola, Puerto Rico, and Jamaica. In conjunction with rate estimates under the best-fit model, these results imply equilibrium or near-equilibrium conditions on Puerto Rico, Hispaniola, and Jamaica; speciation rates on each island have declined to a small fraction of the inferred initial rate (Fig. 1). Only the largest island, Cuba, appears to have potential for substantial species accumulation. Our results further suggest that the rate of decline in speciation through time is negatively correlated with island area: Proportionately more rapid declines occur on smaller islands ($\rho = -0.92$, $P = 0.056$; Fig. 3), suggesting that per-lineage feedback between speciation rates and total species richness is greater on small islands. This negative correlation is robust to uncertainty in phylogenetic tree topology and branch lengths (Fig. S5).

We simulated phylogenetic trees and character state data under maximum-likelihood parameter estimates for GlobalConstant, GlobalVariable, IslandConstant, and IslandVariable models to assess whether the fitted models could reconstruct major features of the observed data. Simulated distributions of species richness under the IslandVariable model were closer to the observed data than alternative models that did not allow island-specific changes in speciation through time (Fig. 4). The GlobalVariable model underpredicts species richness on Cuba relative to the IslandVariable model and overpredicts richness on both Jamaica and Puerto Rico (Fig. 4; Table S3). Analyses of branch length distributions from simulated trees further suggest that the IslandVariable model provides a much better match to the observed data than alternative models specifying global changes in speciation rates or constant speciation through time (Fig. S6). Taken together, these results suggest that models with independent, island-specific changes in speciation rates through time provide a better absolute fit to the observed data than

Table 1. Diversification models specifying dynamic or time-invariant rates of speciation (λ) and extinction (μ) fitted to the maximum clade credibility (MCC) tree for the Greater Antillean *Anolis* radiation

Model	Description	LogL	AIC (np)	AIC_EX (np)	Δ_i
IslandConstant	Rates differ among islands but are constant through time	−40.84	93.68 (6)	101.7 (10)	0
GlobalConstant	Rates are constant through time and among lineages	−43.81	93.62 (3)	95.6 (4)	0
GlobalVariable	Linear change in rates through time; no differences between islands	−32.12	72.24 (4)	74.8 (6)	0.005
IslandVariableFull	Island-specific linear change in rates through time	−22.36	64.72 (10)	74.08 (18)	0.184
IslandVariable	Island-specific linear change in rates through time; shared r_0 (λ_0, μ_0)	−23.96	61.92 (7)	66.58 (12)	0.811

LogL and AIC give log-likelihoods and AIC scores for models formulated without extinction (μ = 0), and AIC_EX gives the corresponding AIC for the models with extinction (μ ≥ 0). The number of parameters in each model (np) is given in parentheses after the AIC score. Δ_i: conditional probability of the *i*th model given the candidate set of models. Models without extinction (μ = 0) fit the data better than the corresponding model with extinction in all cases.

models assuming constant rates through time or global changes in the rate of speciation.

Discussion

The extent to which biological diversity is regulated by diversity-dependent, equilibrium processes relative to diversity-independent, nonequilibrium processes is a fundamental question in evolutionary ecology. Our results provide evidence for parallel declines in speciation rates in radiations of *Anolis* lizards on the four major islands of the Greater Antilles. These results are consistent with a diversity-dependent model involving a decline in speciation rates as species richness and ecological disparity increase (5, 19, 20, 31, 33, 34), possibly reflecting a role for ecological opportunity as a driver of speciation in Caribbean anoles (35, 36). Recent work suggesting that diversification of phenotypic traits associated with ecological specialization also declined through time during the anole radiation further supports this scenario (29, 37).

Our results further suggest that three of four islands are at or near equilibrium diversity and that equilibrium diversity is a function of island area (Fig. 3). One explanation for the higher diversity on larger islands involves the presence of multiple ecologically similar species occurring in geographic isolation; for example, both Cuba and Hispaniola harbor multiple species of montane twig and trunk-crown ecomorph anoles that are endemic to isolated mountain ranges (30). Larger islands also support more species specialized for geographically distinct macrohabitats. Hispaniola, for example, is home to eight species of allopatrically or parapatrically distributed trunk-ground anoles restricted to distinctly different forest types (e.g., montane, lowland mesic, and lowland xeric). A third aspect of increased diversity on larger islands appears to involve finer-scale partitioning of habitats available across islands of all sizes (30); sympatric anole assemblages on Cuba and Hispaniola, for example, may contain more species than the entire island-wide fauna of Jamaica (38).

Our analyses reject models that posit a shared decline in diversification rates across islands in favor of alternative models where speciation dynamics vary among subtrees assigned to dif-

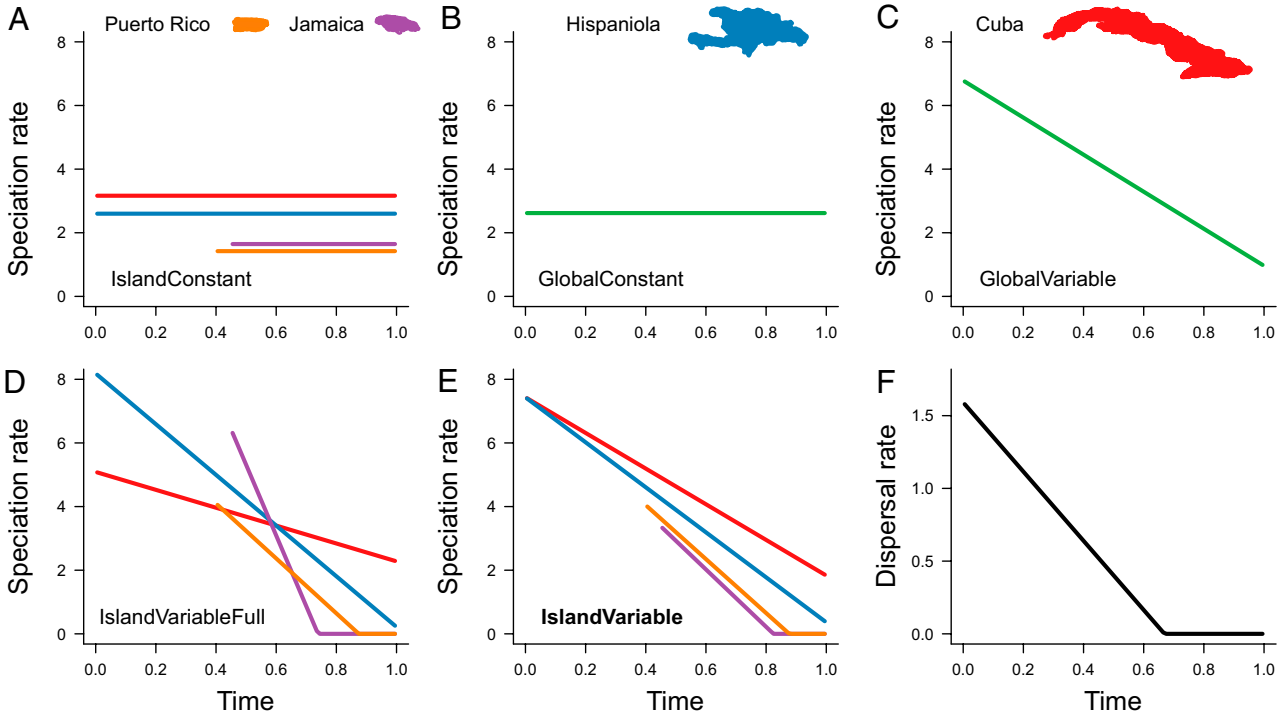

Fig. 1. (*A*–*E*) Reconstructed speciation-through-time curves under five diversification models fitted to the *Anolis* phylogeny (Fig. 2, Fig. S1). Green curves denote models without state-dependent diversification; other colors describe speciation dynamics on Cuba, Hispaniola, Jamaica, and Puerto Rico. Models are sorted (left to right, top to bottom) from lowest to highest conditional probability (Table 1). Models with island-specific changes in speciation (*D* and *E*) account for *P* = 0.995 of the total probability of the data taken across all models. The maximum-likelihood estimate of the dispersal rate between islands under the IslandVariable model is shown in *F*. Rates are shown in relative time units, as the tree was scaled to basal divergence of 1.0.

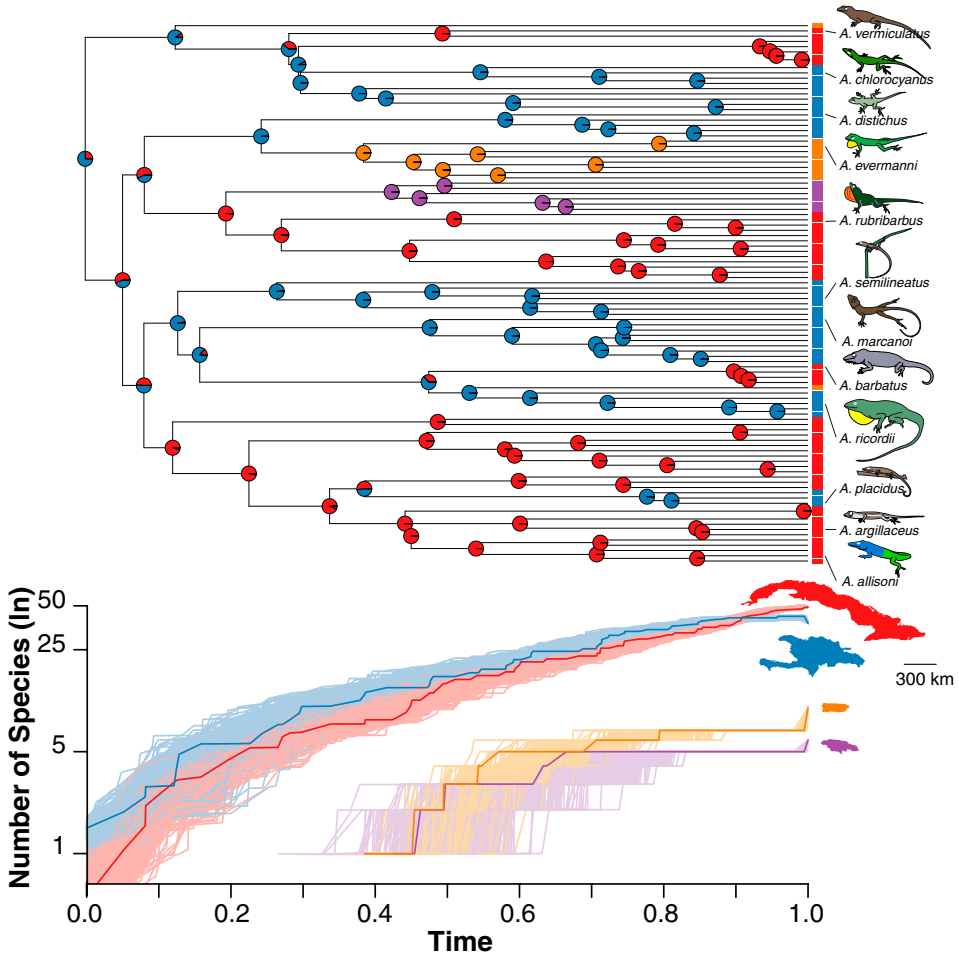

Fig. 2. *Anolis* MCC tree with reconstructed island occupancy probabilities and lineage accumulation curves for Cuba (red), Hispaniola (blue), Jamaica (purple), and Puerto Rico (orange). Occupancy probabilities on internal nodes were estimated under the overall best-fit model (IslandVariable). The MCC tree with all taxon labels is shown in Fig. S1.

ferent islands (Table 1) and add an important dimension to the interpretation of diversification patterns typically seen in molecular phylogenies (19, 20, 39, 40). A criticism of diversity-dependent speciation, as inferred from molecular phylogenies, is that this pattern might simply be an artifact of phylogeny reconstruction or taxon sampling. For example, use of inadequate models of molecular evolution can lead to apparent slowdowns in the rate of speciation through time (32), but phylogenies affected by this bias should not have been favored by models with island-specific speciation dynamics. Likewise, if *Anolis* contains additional cryptic species diversity that has not been accommodated by our analyses, we would observe an artifactual slowdown in speciation toward the present in the full *Anolis* phylogeny. However, such incomplete sampling would require proportionately greater cryptic diversity on the smallest islands, which have undergone the most severe slowdown in speciation through time (Fig. 3). This pattern of undersampling is unlikely given the considerable attention received by Puerto Rican and Jamaican anole faunas relative to those of Cuba; despite this work, no new species have been described on either island since the 1960s, whereas new species continue to accumulate on Cuba (30).

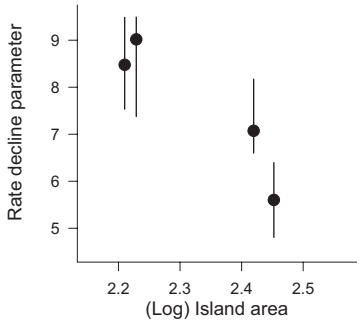

Fig. 3. Island-specific rate-decline parameters as a function of island area for (from left to right) Puerto Rico, Jamaica, Hispaniola, and Cuba. The rate decline parameter is the slope of the relationship between speciation and time ($-\lambda_0/K$). Confidence intervals reflect uncertainty in tree reconstruction and represent the 0.025 and 0.975 percentiles of the distribution of parameter estimates taken across the posterior distribution of trees sampled with BEAST.

Elucidating the role of extinction from molecular phylogenies is notoriously difficult (41–44). However, among anole lineages that left present-day descendants, extinction appears to have been negligible, and our results suggest that the decline in net diversification rates on each island has been mediated by declining speciation rates against a background of very low extinction. There is no evidence from explicit modeling of extinction rates (Table 1 and Table S2) or from visual inspection of lineage accumulation plots (Fig. 2) for substantial species turnover during the historical occupancy of each island. It is possible that many species have gone extinct, but the dominant signal is of a tendency

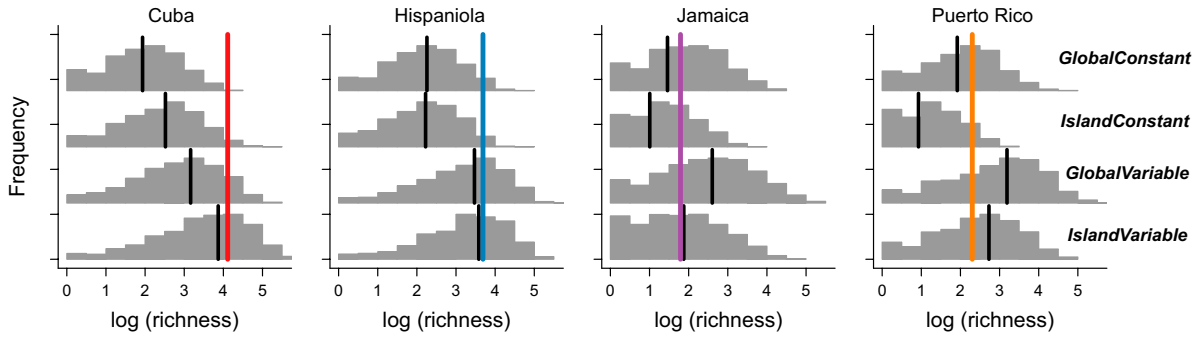

Fig. 4. Distribution of species richness for islands of the Greater Antilles predicted under (*Top* to *Bottom*) GlobalConstant, IslandConstant, GlobalVariable, and IslandVariable models. Colored lines denote observed species richness on each island; black lines and histograms represent mean values and distributions tabulated from 2,000 datasets simulated under maximum-likelihood parameter estimates for each model. The GlobalVariable model underpredicts species richness on Hispaniola and overpredicts richness on both Jamaica and Puerto Rico relative to the IslandVariable model.

for lineages that arose during the earliest stage of each island's radiation to persist to the present: Any subsequent extinction events have failed to leave a signature that can be inferred from molecular phylogenies. This result is consistent with previous analyses that have documented a tendency for major ecological types to have arisen early during the radiation of anoles on each island (29). Such a pattern might be expected if there are strong ecological limits on species diversity and if species tend to give rise to ecologically similar species. Even if extinction rates are high, comparatively little phylogenetic turnover within island communities would occur once diversity reached saturation, because any particular extinction event would be followed by a speciation event from an ecologically similar member of the same major lineage.

When all Caribbean *Anolis* communities are considered together (7), our results imply that communities assembled through speciation have proportionately greater equilibrium diversities than are attained when immigration is the sole source of new species. This hypothesis follows from the observation that the slope of the species–area curve for Caribbean anoles is greater for islands with appreciable in situ speciation (7) than for immigration-derived island assemblages; qualitatively similar patterns occur in Caribbean butterflies (2). This result is not simply a manifestation of the "small island effect," whereby demographic stochasticity on smaller islands may eliminate the expected relationship between island area and species richness (2); rather, immigration-derived anole communities show a positive species–area relationship (7, 25). Further support for this pattern follows from the observation that the slope of the species–area relationship for oceanic archipelagoes is positively correlated with mean island endemicity (45). It is unclear why the scaling relationship between area and equilibrium diversity might change when speciation becomes the dominant contributor to regional diversity, but these observations suggest fundamental differences between communities assembled through speciation and immigration/dispersal.

The variation in species richness among geographic regions, such as the islands we consider here, potentially results from differences in rates of species diversification (11, 13, 46) as well as the ages of constituent clades (12, 47). With the possible exception of Cuba, our results argue against these nonequilibrium processes and suggest that anole species richness is primarily determined by island-specific limits on total diversification (14). These findings have implications for how we study the variation in species richness among geographic regions: If faunas derived principally from in situ speciation typically reach steady-state diversity, then variation in species richness must result in large part from ecological interactions (3) and not necessarily from variation in clade age and net rates of species diversification (14, 48–50).

Materials and Methods

Phylogeny Reconstruction. We analyzed ultrametric phylogenetic trees generated by Mahler et al. (29), consisting of 189 species and comprising an ~1,500-bp region of mitochondrial DNA extending from the beginning of the NADH dehydrogenase subunit 2 (ND2) gene and including five tRNAs before ending shortly after the start of the cytochrome c oxidase (COI) gene (see *SI Materials and Methods* for details). We fit all diversification models to 400 trees sampled without replacement from the set of pruned trees generated by Mahler et al.'s BEAST analyses.

Diversification Analyses and Biogeographic Model Selection. The modeling framework described here allows for an extremely large candidate set of models and poses a challenging combinatorial problem. Even with simple linear changes in parameters through time, we must potentially consider 8 speciation rates (e.g., initial and final rates for each of four islands), 8 extinction rates, and 24 dispersal rates (12 initial rates and 12 final rates). Rather than consider hundreds of possible biogeographic models, we evaluated 12 key models against a diversification background of time-constant but island-specific differences in speciation (see *SI Materials and Methods* for details; Table S1, Fig. S3). These models included a simple 1-parameter symmetric scenario with equal rates between all island pairs, a 2-parameter symmetric model with rates changing linearly through time, and a full 12-parameter asymmetric model. The best-fit model from this analysis (Table S1) was selected as a background model for all subsequent diversification analyses and allowed only the following transitions: q_{21}, q_{12}, q_{13}, and q_{24} (Cuba, 1; Hispaniola, 2; Jamaica, 3; Puerto Rico, 4). Note that dispersal parameters were estimated separately for each diversification model shown in Table 1. Virtually identical results for diversification were obtained when we considered simpler alternative biogeographic models (Table S2). We accounted for incomplete sampling by setting initial states $D_i(0)$ and $E_i(0)$ equal to f_i and $1 - f_i$, where f_i is the proportion of species on island i that have been sampled (26). For models with extinction, extinction functions through time were mirror images of those used for speciation. For example, GlobalConstant with extinction had time-invariant rates λ and μ for all lineages, and IslandVariable with extinction had a common μ_0 term and separate K terms for each island. Additional details are given in *SI Materials and Methods*.

Model Adequacy and Comparisons. We used Akaike weights to estimate the probability of each model conditional on the Akaike Information Criterion (AIC) scores observed in the candidate set of models (51). See *SI Materials and Methods* for details. To assess model adequacy, we developed a continuous-time phylogenetic tree simulation program in R to generate trees and character state data under all SSE models described here. We simulated 2,000 trees under maximum-likelihood parameter estimates for GlobalConstant, IslandConstant, GlobalVariable, and IslandVariable models and computed a series of summary statistics to assess the match between the simulated data and the *Anolis* MCC tree. We tabulated the numbers of species in each character state at the end of the simulation, to determine whether simulated patterns of species richness matched those observed in the Greater Antilles (Fig. 4). We then computed two summary statistics that described the distribution of branch lengths associated with particular island states: the mean and coefficient of variation in terminal branch lengths associated with each character state (*SI Materials and Methods*; Fig. S6). The best-fit model (IslandVariable) outperformed the other candidate models for all three summary statistics.

ACKNOWLEDGMENTS. We thank A. Agrawal, J. Huelsenbeck, I. Lovette, A. McCune, A. Phillimore, R. Ricklefs, K. Wagner, and members of the Glor lab for comments on the manuscript and/or discussion of these topics. This research was supported by US National Science Foundation Grants DEB-0814277 and DEB-0920892, by the Fuller Evolutionary Biology Program at the Cornell Laboratory of Ornithology, by the University of Rochester, and by the Miller Institute for Basic Research in Science at University of California, Berkeley.

1. MacArthur RH, Wilson EO (1967) *The Theory of Island Biogeography* (Princeton Univ Press, Princeton).
2. Lomolino MV (2000) Ecology's most general, yet protean pattern: The species-area relationship. *J Biogeogr* 27:17–26.
3. MacArthur RH (1969) Patterns of communities in the tropics. *Biol J Linn Soc Lond* 1: 19–30.
4. Losos JB, Ricklefs RE, eds (2010) *The Theory of Island Biogeography Revisited* (Princeton Univ Press, Princeton).
5. Rosenzweig ML (1995) *Species Diversity in Space and Time* (Cambridge Univ Press, Cambridge, UK).
6. Fine PVA, Ree RH (2006) Evidence for a time-integrated species-area effect on the latitudinal gradient in tree diversity. *Am Nat* 168:796–804.
7. Losos JB, Schluter D (2000) Analysis of an evolutionary species-area relationship. *Nature* 408:847–849.
8. Parent CE, Crespi BJ (2006) Sequential colonization and diversification of Galapagos endemic land snail genus *Bulimulus* (Gastropoda, Stylommatophora). *Evolution* 60: 2311–2328.
9. Benton MJ, Emerson BC (2007) How did life become so diverse? The dynamics of diversification according to the fossil record and molecular phylogenetics. *Paleontology* 50:23–40.
10. Kisel Y, Barraclough TG (2010) Speciation has a spatial scale that depends on levels of gene flow. *Am Nat* 175:316–334.
11. Mittelbach GG, et al. (2007) Evolution and the latitudinal diversity gradient: Speciation, extinction and biogeography. *Ecol Lett* 10:315–331.
12. Stephens PR, Wiens JJ (2003) Explaining species richness from continents to communities: The time-for-speciation effect in emydid turtles. *Am Nat* 161:112–128.
13. Weir JT, Schluter D (2007) The latitudinal gradient in recent speciation and extinction rates of birds and mammals. *Science* 315:1574–1576.
14. Rabosky DL (2009) Ecological limits and diversification rate: Alternative paradigms to explain the variation in species richness among clades and regions. *Ecol Lett* 12: 735–743.
15. Raup DM (1972) Taxonomic diversity during the Phanerozoic. *Science* 177:1065–1071.
16. Sepkoski JJ (1978) A kinetic model of Phanerozoic taxonomic diversity I. Analysis of marine orders. *Paleobiology* 4:223–251.
17. Alroy J, et al. (2008) Phanerozoic trends in the global diversity of marine invertebrates. *Science* 321:97–100.
18. Walker TD, Valentine JW (1984) Equilibrium models of evolutionary species diversity and the number of empty niches. *Am Nat* 124:887–899.
19. Phillimore AB, Price TD (2008) Density dependent cladogenesis in birds. *PLoS Biol* 6: e71.
20. Rabosky DL, Lovette IJ (2008) Density dependent diversification in North American wood warblers. *Proc Biol Sci* 275:2363–2371.
21. Gillespie R (2004) Community assembly through adaptive radiation in Hawaiian spiders. *Science* 303:356–359.
22. Gillespie R, Baldwin BG (2010) Island biogeography of remote archipelagoes. *The Theory of Island Biogeography Revisited*, eds Losos JB, Ricklefs RE (Princeton Univ Press, Princeton), pp 358–387.
23. Sax DF, Gaines SD, Brown JH (2002) Species invasions exceed extinctions on islands worldwide: A comparative study of plants and birds. *Am Nat* 160:766–783.
24. Ricklefs RE, Lovette IJ (1999) The roles of island area per se and habitat diversity in the species-area relationships of four Lesser Antillean faunal groups. *J Anim Ecol* 68: 1142–1160.
25. Losos JB, Parent CE (2010) The speciation-area relationship. *The Theory of Island Biogeography Revisited*, eds Losos JB, Ricklefs RE (Princeton Univ Press, Princeton), pp 415–438.
26. FitzJohn R, Maddison WP, Otto SP (2009) Estimating trait-dependent speciation and extinction rates from incompletely resolved phylogenies. *Syst Biol* 58:595–611.
27. Maddison WP, Midford PE, Otto SP (2007) Estimating a binary character's effect on speciation and extinction. *Syst Biol* 56:701–710.
28. FitzJohn R (2010) Quantitative traits and diversification. *Syst Biol* 59:619–633.
29. Mahler DL, Revell LJ, Glor RE, Losos JB (2010) Ecological opportunity and the rate of morphological evolution in the diversification of Greater Antillean anoles. *Evolution* 64:2731–2745.
30. Losos JB (2009) *Lizards in an Evolutionary Tree: Ecology and Adaptive Radiation of Anoles* (Univ of California Press, Berkeley).
31. Rabosky DL, Lovette IJ (2008) Explosive evolutionary radiations: Decreasing speciation or increasing extinction through time? *Evolution* 62:1866–1875.
32. Revell LJ, Harmon LJ, Glor RE (2005) Underparameterized model of sequence evolution leads to bias in the estimation of diversification rates from molecular phylogenies. *Syst Biol* 54:973–983.
33. Nee S, Mooers A, Harvey PH (1992) Tempo and mode of evolution revealed from molecular phylogenies. *Proc Natl Acad Sci USA* 89:8322–8326.
34. Rosenzweig ML (1975) On continental steady states of species diversity. *Ecology and Evolution of Communities*, eds Cody ML, Diamond JM (Belknap, Cambridge, MA), pp 121–140.
35. Losos JB, Mahler DL (2010) Adaptive radiation: The interaction of ecological opportunity, adaptation, and speciation. *Evolution Since Darwin: The First 150 Years*, eds Bell M, Futuyma DJ, Eanes WF, Levinton JS (Sinauer, Sunderland, MA), pp 381–420.
36. Yoder JB, et al. (2010) Ecological opportunity and the origin of adaptive radiations. *J Evol Biol* 23:1581–1596.
37. Harmon LJ, Schulte JA, Larson A, Losos JB (2003) Tempo and mode of evolutionary radiation in iguanian lizards. *Science* 301:961–964.
38. Losos JB, et al. (2003) Niche lability in the evolution of a Caribbean lizard community. *Nature* 424:542–545.
39. McPeek MA (2008) Ecological dynamics of clade diversification and community assembly. *Am Nat* 172:E270–E284.
40. Ruber L, Zardoya R (2005) Rapid cladogenesis in marine fishes revisited. *Evolution* 59: 1119–1127.
41. Quental TB, Marshall CR (2009) Extinction during evolutionary radiations: Reconciling the fossil record with molecular phylogenies. *Evolution* 63:3158–3167.
42. Quental TB, Marshall CR (2010) Diversity dynamics: Molecular phylogenies need the fossil record. *Trends Ecol Evol* 25:434–441.
43. Rabosky DL (2009) Heritability of extinction rates links diversification patterns in molecular phylogenies and fossils. *Syst Biol* 58:629–640.
44. Rabosky DL (2010) Extinction rates should not be estimated from molecular phylogenies. *Evolution* 64:1816–1824.
45. Triantis KA, Mylonas M, Whittaker RJ (2008) Evolutionary species-area curves as revealed by single-island endemics: Insights for the inter-provincial species-area relationship. *Ecography* 31:401–407.
46. Moore BR, Donoghue MJ (2007) Correlates of diversification in the plant clade dipsacales: Geographic movement and evolutionary innovations. *Am Nat* 170: S28–S55.
47. Ricklefs RE (2006) Global variation in the diversification rate of passerine birds. *Ecology* 87:2468–2478.
48. Rabosky DL (2009) Ecological limits on clade diversification in higher taxa. *Am Nat* 173:662–674.
49. Ricklefs RE (2007) Estimating diversification rates from phylogenetic information. *Trends Ecol Evol* 22:601–610.
50. Ricklefs RE (2009) Speciation, extinction, and diversity. *Speciation and Patterns of Diversity*, eds Butlin R, Bridle J, Schluter D (Cambridge Univ Press, Cambridge, UK), pp 257–277.
51. Burnham KP, Anderson DR (2002) *Model Selection and Multimodel Inference—A Practical Information-Theoretic Approach* (Springer, New York).

Supporting Information

Rabosky and Glor 10.1073/pnas.1007606107

SI Materials and Methods

Phylogenetic Methods. Phylogenetic trees were generated by Mahler et al. (1). Mahler et al. conducted multiple partitioned analyses in MrBayes v3.1.2; the consensus tree from these analyses was then used as the starting tree for the Bayesian relaxed clock method implemented in BEAST 1.4.7. All non-Greater Antillean taxa were then pruned from the trees in the posterior distribution of the BEAST analysis.

Diversification Analyses. The equations for modeling state-dependent diversification dynamics follow from Maddison et al. (2), and we used simple modifications of the original equations. The reader is referred to the original paper for a clear and detailed explanation of the derivation of the two-state BiSSE model (2). In this framework, we track—for each character state—two key probabilities: $D_i(t)$, the probability that a lineage in state i at time t gives rise to a clade like that in the observed data; and $E_i(t)$, the probability that a lineage in state i at time t goes extinct before the present (along with all of its descendants). Here, t is time measured from the present backward in time and Δt is an incremental time step. Let $\lambda_{i,t}$ and $\mu_{i,t}$ be the speciation and extinction rates for a lineage in state i at time t and $q_{ij,t}$ represent the rate of transition from state i to state j at time t. As in Maddison et al. (2) and FitzJohn et al. (3), we assume that only a single event (speciation, extinction, or character change) can happen in the interval Δt. The differential equation governing $D_i(t + \Delta t)$ is

$$\frac{dD_i}{dt} = -\left(\mu_{i,t} + \lambda_{i,t} + \sum_{j=1}^{j\neq i} q_{ij,t}\right)D_i(t) + \sum_{j=1}^{j\neq i} q_{ij,t}D_j(t) + 2\lambda_{i,t}E_i(t)D_i(t),$$

where

$$-\left(\mu_{i,t} + \lambda_{i,t} + \sum_{j=1}^{j\neq i} q_{ij,t}\right)$$

is the rate at which $D_i(t)$ decreases due extinction, speciation, or character change (from state i to all other states) in some infinitesimal amount of time Δt as we move backward down the branch (toward the root), and

$$q_{ij,t}D_j(t)$$

is the rate at which $D_i(t)$ increases due to character change from state i to state j [multiplied by the probability that, having undergone character change, the lineage will go on to evolve into a clade like the observed data, $D_j(t)$]. This term must be summed over all $n - 1$ character states, hence the summation term. Finally, a lineage at some point in time can undergo a speciation event and still give rise to the observed data, provided one of the descendant branches and all of its descendants go extinct before the present (thus, we would never observe a speciation event in a reconstructed tree). This process occurs with rate

$$\lambda_{i,t}E_i(t)D_i(t)$$

and it must be multiplied by 2 (as either the left or the right descendant branches and all their descendants could go extinct, if there is a speciation event on Δt).

The differential equation governing $E_i(t)$ is

$$\frac{dE_i}{dt} = \mu_{i,t} - \left(\mu_{i,t} + \lambda_{i,t} + \sum_{j=1}^{j\neq i} q_{ij,t}\right)E_i(t) + \sum_{j=1}^{j\neq i} q_{ij,t}E_j(t) + \lambda_{i,t}E_i(t)^2$$

and includes the rate at which lineages go extinct on Δt, or $\mu_{i,t}$. The equation includes the rate at which lineages undergo no events on the time interval δt, yet go extinct at some point in the future, or

$$\mu_{i,t} + \lambda_{i,t} + \sum_{j=1}^{j\neq i} q_{ij,t}$$

plus the rate at which lineages in state i switch states and subsequently go extinct, or

$$q_{ij,t}E_j(t),$$

which must be summed over all n character states. Finally, a lineage might undergo speciation on Δt, but for such an event to occur and yet result in a clade that goes extinct before the present, both descendant branches and all their descendants must go extinct. These events occur at rate

$$\lambda_{i,t}E_i(t)^2.$$

A total of $2n$ equations must thus be solved simultaneously to describe the dynamics of diversification and character change through time. The initial conditions, for a tree with complete taxon sampling, are $D_i(0) = 1$ and $E_i(0) = 0$. The probability that a lineage existing in the present will give rise to the observed data—a single lineage—is necessarily 1, unless we are accounting for incomplete taxon sampling. In this case, the initial state is simply the probability of sampling the lineage (3). We solved these systems of equations by numerically integrating backward along each branch using the Fortran LSODA integrator as implemented in the R package deSolve (4). At each interior node in the tree, probabilities $D_i(t)$ for right and left descendant branches were combined as in Maddison et al. (2), and these combined values became the initial conditions for integration backward down the parent branch. At the root node, we combined root-state probabilities using the weighting scheme from FitzJohn et al. (3). Virtually identical results were obtained using alternative weighting methods that assumed equal weights to the individual probabilities $D_1, D_2, \ldots, D_n$.

Biogeographic Model Selection. A large number of biogeographic scenarios could be considered to model transitions between character states (e.g., dispersal between islands). Under the simplest model, dispersal (transition) rates between all islands might be identical. This model would specify a symmetric, one-rate transition matrix between states. At the most complex end of the spectrum, each pair of character states might have separate asymmetric transition rates ($q_{ij} \neq q_{ji}$), and all rates might vary linearly through time. This model would have a full 24-parameter transition matrix between character states (12 initial rates at the root node and 12 ending rates in the present). Between these scenarios, a very large number of models are possible. We used the state-dependent diversification framework described above and subsequent model-fitting analyses to identify an appropriate background model for subsequent diversification analyses, rather than simply assuming the validity of a one-rate symmetric transition matrix or any other model.

We assumed that all character states (islands) were associated with a particular time-constant rate of speciation, with extinction set to zero. We then used maximum likelihood to fit three biogeographic models to the *Anolis* MCC tree: (*i*) a model with time-invariant, equal rates between all islands (1 parameter, model qsymm1); (*ii*) a model with time-varying dispersal between islands, but with a single rate for all islands at any point in time (2 parameters, model qsymm1_TD); and (*iii*) a model with separate asymmetric transition rates between all island pairs, with rates constant in time (12 parameters, model qasymm12). Many entries in the 12-parameter transition matrix were estimated as zero with a high degree of confidence, owing to the clear lack of obvious dispersal events between many island pairs (e.g., Jamaica and Puerto Rico).

We thus generated a series of secondary "dropped-zero" transition matrices by dropping all of the estimated zero entries in the 12-parameter model. Our analyses of the 12-parameter model recovered two stable solutions that differed in <0.5 log-likelihood units: (*i*) a model with two-way dispersal between Cuba and Hispaniola and one-way dispersal from Cuba to Jamaica and from Hispaniola to Puerto Rico, with all other rates equal to zero (model suffix ch/hc/cj/hp); and (*ii*) an "out of Cuba" model with one-way dispersal from Cuba to all other islands, with all other rates equal to zero (model suffix cuba). We considered a third dropped-zero model by essentially merging these two models, thus generating (*iii*) a model that allowed dispersal from Cuba to all other islands and from Hispaniola to all other islands (model suffix ch:hc).

For all of these secondary dropped-zero models, we considered the following scenarios: (*i*) a one-rate constant, time-invariant rate for all nonzero rate entries of the rate matrix (1 parameter), (*ii*) a *k*-rate model with separate time-invariant rates between all nonzero entries of the rate matrix (*k* parameters), and (*iii*) a model with a single rate that varied through time for all nonzero entries of the matrix (two parameters). All 12 of these models are illustrated in Fig. S3.

Of all models we considered, the greatest improvement in model likelihoods came from simply relaxing the assumption of time-invariant dispersal between islands (Table S1). For example, the log-likelihood of the 12-parameter time-invariant model (qasymm12) was −48.78, yet a simple 2-parameter model with equal rates between all island pairs at any point in time (qsymm1_TD) had a much higher log-likelihood (−42.68). The overall best model was the 2-parameter dropped-zero model allowing only dispersals between Cuba and Hispaniola and from Cuba to Jamaica and from Hispaniola to Puerto Rico. Results using this model as a biogeographic background model are shown in Table 1.

We recognize that our inference about diversification processes is conditional on the underlying biogeographic model used to account for transitions between character states. Ideally, one would consider all possible biogeographic models—of which there are 12, each with 10 diversification models—leading to a minimum of 120 diversification/biogeographic model combinations to be considered. Rather than consider all possible models, we fit the 10 diversification models (Table 1) against two simpler biogeographic models to verify that our results were not simply a function of choosing the qsmm.ch/hc/cj/hp_TD model (Fig. S3). These results, using the poor-fitting one-rate symmetric model (qsymm1) and the much better time-varying model qsymm1_TD provided nearly identical results to those given in Table 1, indicating that our results are not sensitive to the underlying biogeographic model used for inference. These results are summarized in Tables S2 and S3.

Ancestral State Reconstruction and Lineage Accumulation Curves. Ancestral state (island occupancy) probabilities are essentially computed during the implementation of the model described above. At each node in the phylogeny, the probabilities $D_i(t)$ for each descendant branch are combined. By normalizing these state probabilities, we obtain an estimate of the probability that a given node k was in any of the N possible character states. The probability that node k is in state i is given by

$$p_{k,i} = \frac{D_{i,k}}{\sum_{j=1}^{N} D_{j,k}}.$$

We used these node probabilities to estimate lineage accumulation curves for each island (Fig. 2). The approximate number of lineages in state i at time T is then given by

$$\Phi_{T,i} = \sum_{j=1}^{B} p_{j,i} z_j,$$

where $p_{k,i}$ is the probability of state k at node i and z is an indicator variable; and $z_i = 0$ if node i is younger than node x (e.g., $t > T$) and 1 otherwise (B is the total number of nodes).

Evaluation of Model Adequacy. To assess whether the fitted models could recover patterns of species richness and branch lengths consistent with those observed for *Anolis*, we simulated phylogenetic trees and character state data under maximum-likelihood parameter estimates for GlobalConstant, IslandConstant, GlobalVariable, and IslandVariable models. We then used three summary statistics to test whether predictions under the fitted models match patterns in the observed data. We first simply tabulated the species richness values for each island at the end of each simulation and compared these values to the observed data (Fig. 4 and Table S4).

The remaining statistics we computed assessed patterns of branch length variation in simulated trees. We are most interested in how well branch lengths associated with character state *i* match branch lengths associated with character state *i* in the *Anolis* data. Because we do not know with certainty which internal branch lengths can be assigned to which character state in *Anolis*, we considered only terminal branch lengths. We thus computed the mean terminal branch length for all terminals with character state *i* (Fig. S6), as well as the coefficient of variation in terminal branch lengths (Fig. S7). These results suggest that the best-fit model by likelihood analysis (IslandVariable) consistently fits the observed data for all three summary statistics better than the alternative models with time-invariant diversification or global declines in speciation through time.

Model Comparisons. We used Akaike weights to estimate the conditional probability of each model (5). Given the set of AIC scores corresponding to the M candidate models, we first computed the difference (ΔAIC_i) between each AIC score and the overall best (lowest) AIC score. These quantities are then used to estimate the probability of model i conditional on the AIC scores observed in the candidate set. This probability is

$$\Delta_i = \frac{\exp\left(-\frac{\Delta AIC_i}{2}\right)}{\sum_{k=1}^{M} \exp\left(-\frac{\Delta AIC_k}{2}\right)},$$

where the term in the numerator is known as the Akaike weight of the *i*th model.

1. Mahler DL, Revell LJ, Glor RE, Losos JB (2010) Ecological opportunity and the rate of morphological evolution in the diversification of Greater Antillean anoles. *Evolution* 64:2731–2745.
2. Maddison WP, Midford PE, Otto SP (2007) Estimating a binary character's effect on speciation and extinction. *Syst Biol* 56:701–710.
3. FitzJohn R, Maddison WP, Otto SP (2009) Estimating trait-dependent speciation and extinction rates from incompletely resolved phylogenies. *Syst Biol* 58:595–611.
4. Soetaert K, Petzoldt T, Setzer RW (2009) deSolve: General solvers for initial value problems of ordinary differential equations (ODE), partial differential equations (PDE) and differential algebraic equations (DAE), R package version 1.5Available at http://CRAN.R-project.org/package=deSolve.
5. Burnham KP, Anderson DR (2002) *Model Selection and Multimodel Inference—A Practical Information-Theoretic Approach* (Springer, New York).

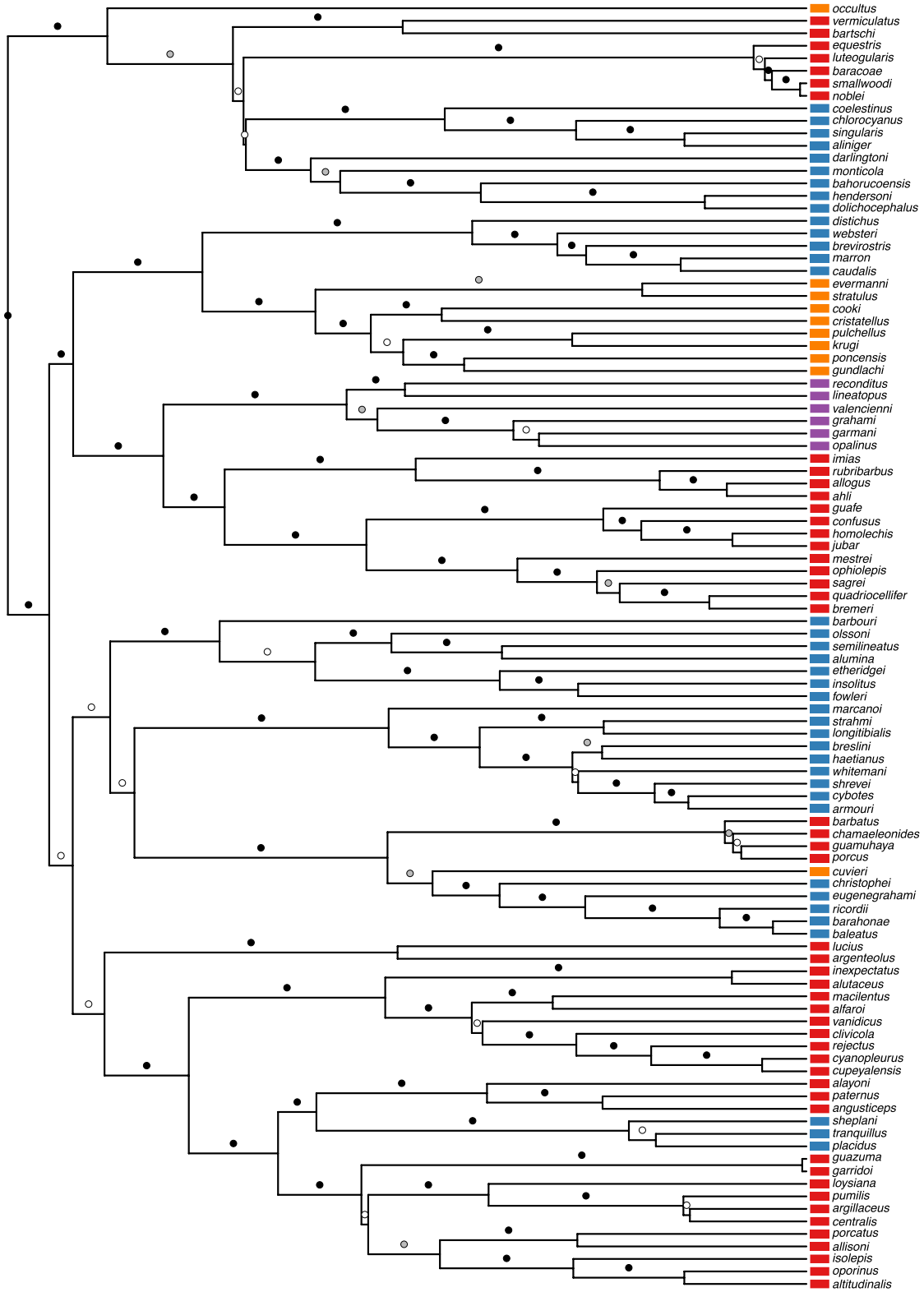

Fig. S1. Maximum clade credibility (MCC) tree resulting from BEAST analyses. Posterior probability (pp) values from the MrBayes analyses used to generate the starting tree for BEAST are indicated by circles above branches (black, pp > 0.95; gray, 0.95 > pp < 0.70; white, pp < 0.70). Island occupancy is indicated across the tips of the tree (green, Cuba; blue, Hispaniola; yellow, Puerto Rico; orange, Jamaica).

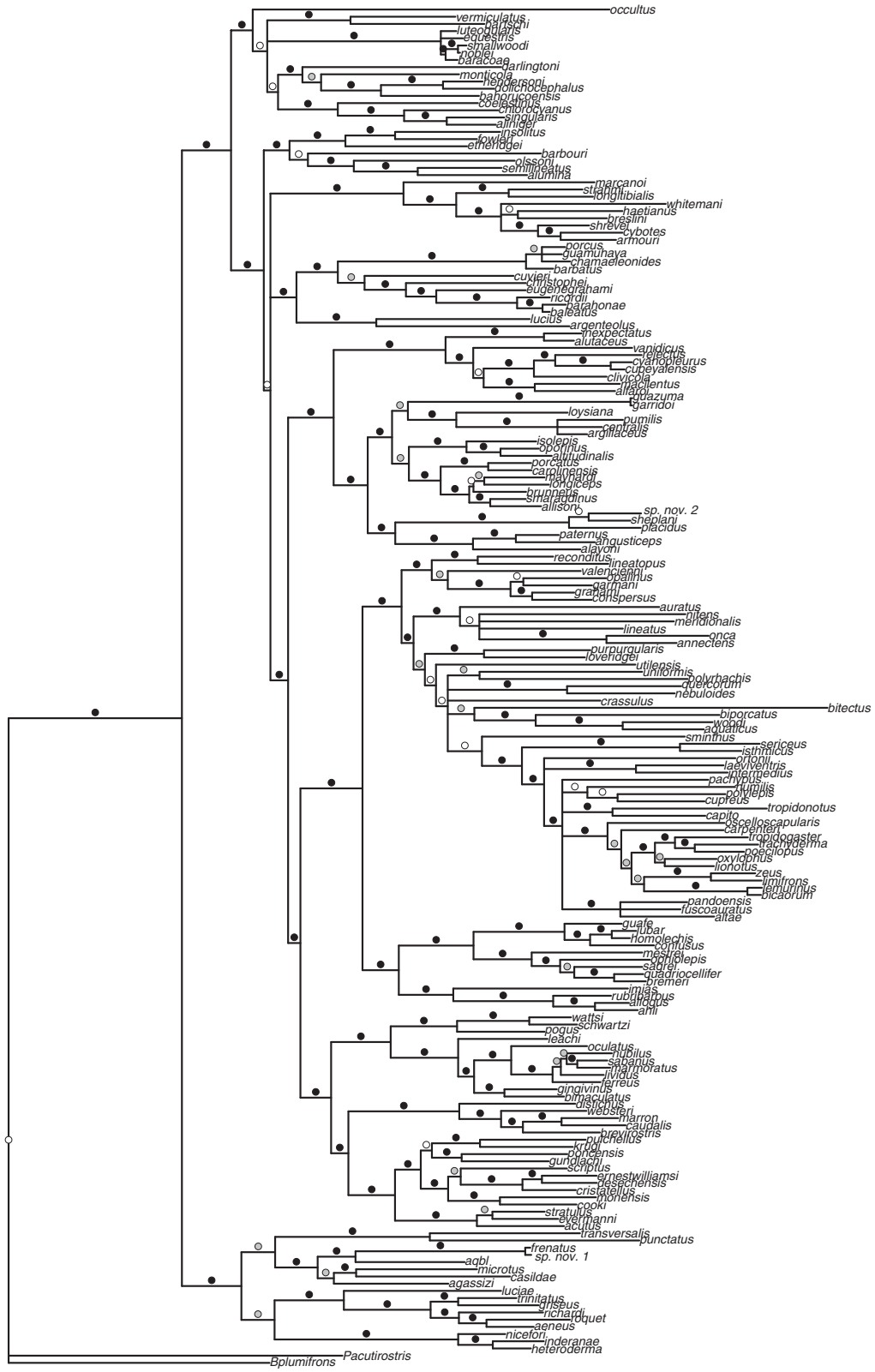

Fig. S2. Consensus tree and branch lengths generated from posterior distribution of MrBayes analysis using the sumt command. This tree includes non-Greater Antillean taxa that were pruned before our analyses. Posterior probability values are indicated by circles above branches (black, pp > 0.95; gray, 0.95 > pp < 0.70; white, pp < 0.70).

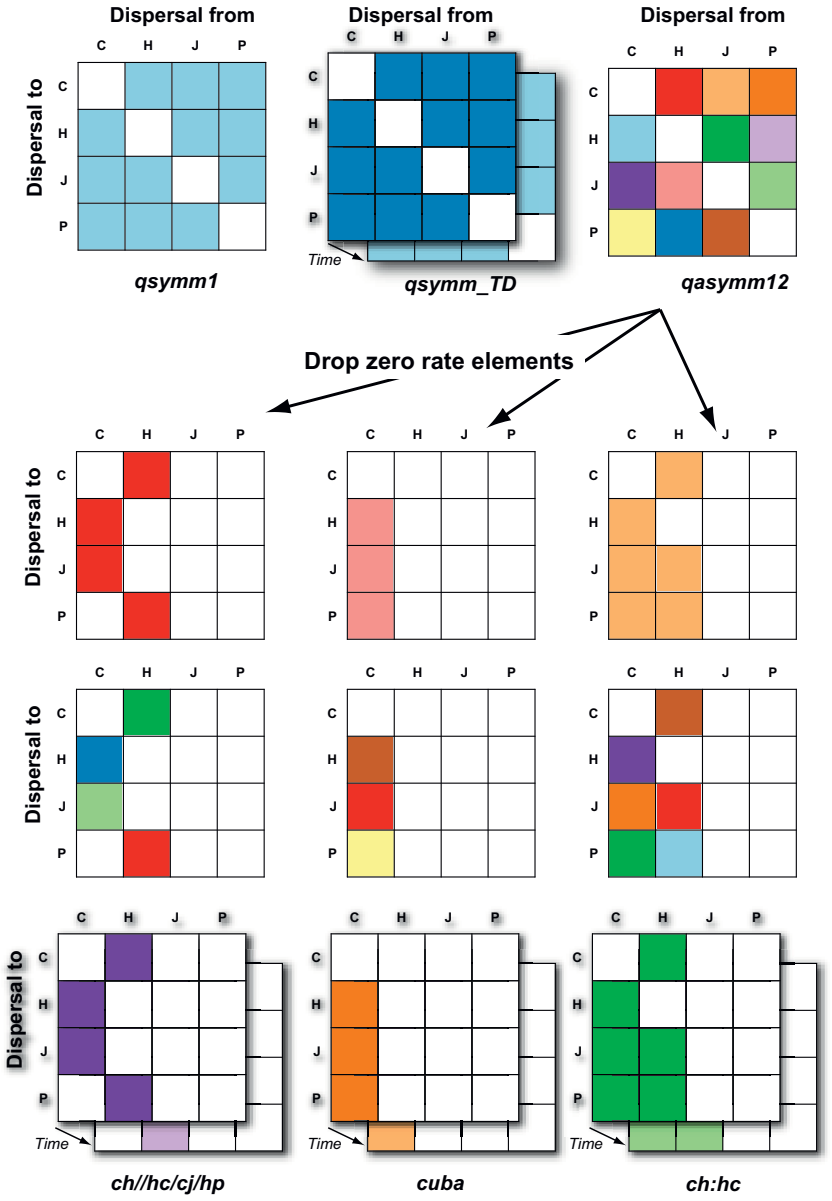

Fig. S3. Biogeographic dispersal models considered for *Anolis*. We considered 12 possible transition matrices representing dispersals between island states. Colored entries denote rate parameters that were free to vary under the model; white entries denote rate parameters that were set equal to zero. Parameters with identical colors are constrained to have the same value (e.g., qsymm1, *Upper Left*, with identical dispersal rates between all islands). The *Lower* three columns of submatrices (ch/hc/cj/hp, cuba, and ch:hc) were formed by eliminating rate parameters from the fitted qasymm12 model if rates under that model were estimated as zero ($<10^{-10}$). Models with time-varying dispersal parameters fitted the data much better than models with time-invariant dispersal (Table S1).

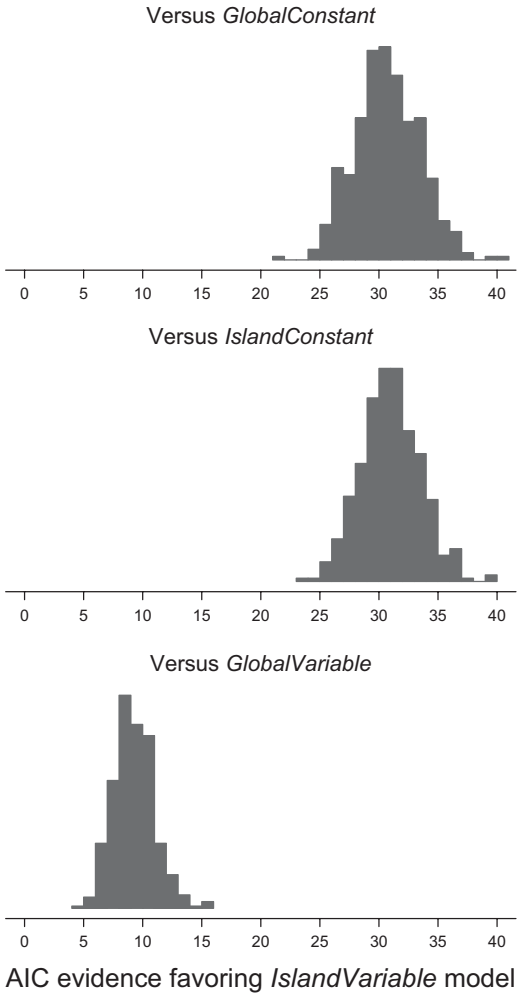

Fig. S4. Robustness of results to phylogenetic uncertainty. Histograms show AIC evidence favoring the IslandVariable model (separate linear change in speciation rates through time on each island) relative to GlobalConstant, IslandConstant, and GlobalVariable models, where all models were fitted to 400 trees sampled randomly from the posterior distributions of trees from the BEAST analysis. The IslandVariable model consistently fits better than GlobalVariable.

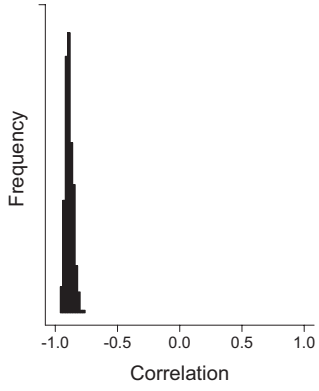

Fig. S5. Pearson correlation between log(island area) and the rate decline parameter ($-\lambda_0/K$) under the best-fit model (IslandVariable) tabulated from 400 trees sampled randomly from the posterior distributions of trees from the BEAST analysis. The rate decline parameter is the slope of the relationship between the speciation rate and time. A negative correlation implies that larger islands have slower changes in speciation rates with respect to time.

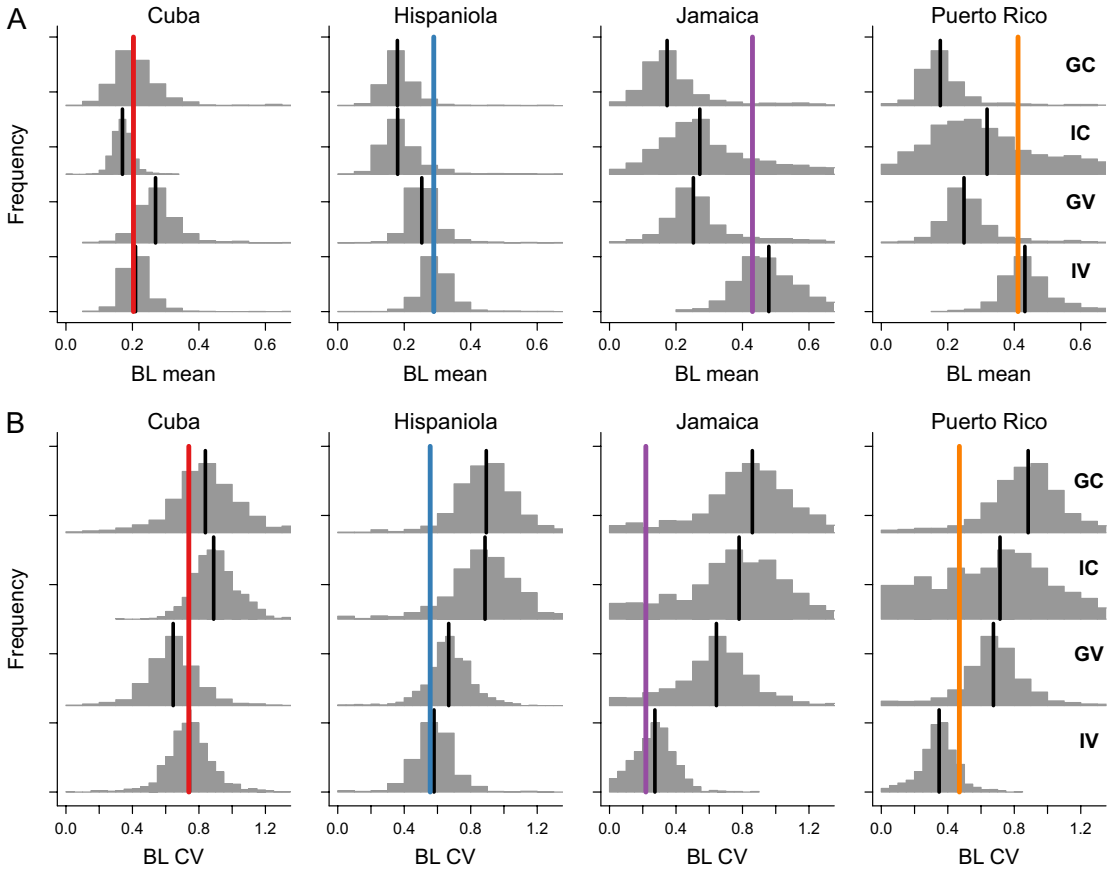

Fig. S6. Distribution of mean terminal branch lengths (*A*) and the coefficient of variation in terminal branch lengths (*B*) for trees simulated under four fitted diversification models, partitioned by terminal character state (Cuba, Hispaniola, Jamaica, or Puerto Rico). Models are (*Top* to *Bottom*) as follows: GC, GlobalConstant; IC, IslandConstant; GV, GlobalVariable; IV, IslandVariable. Colored lines denote mean values for the *Anolis* MCC tree; black lines and histograms represent mean values and distributions tabulated from 2,000 datasets simulated under maximum-likelihood parameter estimates for each model. The IslandVariable model provides a much closer match to the observed data than the three alternative models.

Table S1. Biogeographic models evaluated (see Fig. S2 for graphical description)

Model	Description	np	LogL	AIC	ΔAIC
qasymm12	Asymmetric transition rates between all island pairs.	16	−48.78	129.56	35.88
qsymm1	Single transition rate between all islands.	5	−54.9	119.8	26.12
qsymm.ch:hc	"Out of Cuba/out of Hispaniola" model. Single rate for all transitions from Cuba to all other islands and from Hispaniola to other islands (q_{12}, q_{13}, q_{14}, q_{21}, q_{23}, q_{24}); 0 for all others.	5	−53.9	117.8	24.12
qasymm.ch:hc6	Out of Cuba/out of Hispaniola model. Different rates for q_{12}, q_{13}, q_{14}, q_{21}, q_{23}, q_{24}; 0 for all others.	10	−48.78	117.56	23.88
qsymm.cuba	"Out of Cuba" model. Single rate for q_{12}, q_{13}, q_{14}; 0 for all others.	5	−52.36	114.72	21.04
qasymm.ch/hc/cj/hp.4	Different rates for q_{12}, q_{21}, q_{13}, q_{24} (between Cuba and Hispaniola and from Cuba to Jamaica and from Hispaniola to Puerto Rico); 0 for all others.	8	−48.8	113.6	19.92
qasymm.cuba3	Out of Cuba, with different rates for q_{12}, q_{13}, q_{14}; 0 for all others.	7	−49.67	113.34	19.66
qsymm.ch/hc/cj/hp	Single rate for q_{12}, q_{21}, q_{13}, q_{24}; all other rates 0.	5	−51.4	112.8	19.12
qsymm.ch:hc_TD	Single time-varying transition parameter for all transitions from Cuba and Hispaniola to all other islands.	6	−43.17	98.34	4.66
qsymm1_TD	Single time-varying transition parameter between all islands.	6	−42.68	97.36	3.68
qsymm.cuba_TD	Single time-dependent out of Cuba transition parameter (q_{12}, q_{13}, $q_{14} > 0$); all others = 0.	6	−42.67	97.34	3.66
qsymm.ch/hc/cj/hp_TD	Shared time-varying parameter for q_{12}, q_{21}, q_{13}, q_{24}.	6	−40.84	93.68	0

All biogeographic scenarios were evaluated against a background diversification model with island-specific differences in speciation, but no rate variation through time (IslandConstant model). Models with linear time-dependent change in the transition rate ("TD") fitted the data much better than corresponding models without time-dependent transition rates. States 1, 2, 3, and 4 correspond to Cuba, Hispaniola, Jamaica, and Puerto Rico, respectively.

Table S2. Model-fitting results under alternative biogeographic background models (Table S1: qsymm_TD and qsymm)

Diversification model	NP (μ = 0)	LogL (μ = 0)	ΔAIC (μ = 0)	NP (μ ≥ 0)	LogL (μ ≥ 0)	ΔAIC (μ ≥ 0)	Δ_i
Biogeographic model: Symmetric dispersal between all islands, but rate varies through time (qsymm_TD)							
IslandConstant	6	−42.68	29.88	10	−42.67	37.86	0
GlobalConstant	3	−46.57	31.66	4	−46.56	33.64	0
GlobalVariable	4	−34.87	10.26	6	−34.63	13.78	0.006
IslandVariableFull	10	−25.97	4.46	18	−22.1	12.72	0.091
IslandVariable	7	−26.74	0	12	−24.3	5.12	0.903
Biogeographic model: Symmetric dispersal between all islands, but rate is constant through time (qsymm)							
IslandConstant	5	−54.91	30.04	9	−54.91	38.04	0
GlobalConstant	2	−58.22	30.66	3	−58.19	32.6	0
GlobalVariable	3	−46.58	9.38	5	−45.5	11.22	0.004
IslandVariableFull	9	−38.11	4.44	17	−27.96	0.14	0.460
IslandVariable	6	−38.89	0	11	−35.4	3.02	0.536

All diversification models are identical to those in Table 1. The biogeographic model assumes equal transition rates between all pairs of islands at any point in time, but with (*i*) a linear change in the rate of transitions through time (*Upper* row, *Center*, in Fig. S3), or (*ii*) identical time-invariant rates through time (*Upper* row, *Left*, in Fig. S3). Results are shown for models without (μ = 0) and with (μ ≥ 0) extinction. np, number of parameters; Δ_i, conditional probability of each model given the candidate set of models. Models without extinction (μ = 0) fit the data better than the corresponding model with extinction in all cases but one (IslandVariableFull under qsymm). Models specifying island-specific changes in λ and/or μ account for $P = 0.994$ of the total probability of the data taken across all models, and the GlobalVariable model fits much more poorly than the IslandVariable model.

Table S3. Summary statistics for island species richness in datasets simulated under maximum-likelihood parameters of GlobalConstant, IslandConstant, GlobalVariable, and IslandVariable models (Table 1)

Model	Island	Observed	Mean	Median	q_{25}	q_{75}
GlobalConstant	Cuba	61	6.93	4	0	10
GlobalConstant	Hispaniola	40	9.56	6	1	14
GlobalConstant	Jamaica	6	4.3	0	0	5
GlobalConstant	Puerto Rico	10	6.8	3	0	10
IslandConstant	Cuba	61	12.42	7	0	18
IslandConstant	Hispaniola	40	9.23	6	1	14
IslandConstant	Jamaica	6	2.3735	0	0	4
IslandConstant	Puerto Rico	10	2.53	1	0	4
GlobalVariable	Cuba	61	23.6	15	4	33.25
GlobalVariable	Hispaniola	40	32.17	23	7	47
GlobalVariable	Jamaica	6	13.508	4	0	17
GlobalVariable	Puerto Rico	10	24.284	13	2	35
IslandVariable	Cuba	61	47.8	30	9	69
IslandVariable	Hispaniola	40	35.95	26	10	52
IslandVariable	Jamaica	6	6.5	2	0	8
IslandVariable	Puerto Rico	10	15	9	2	21.5

Observed denotes observed species richness on each island. q_{25} and q_{75} denote 0.25 and 0.75 percentiles of the distribution of richness values under each simulation model.